# Effect of Swept Angle on Aerodynamic Force Generation of a Swept Twist Round (STR) Vertical Blade

**Nanang Mahardika**
Pishon Energy, Jeongwang 1268-12, Siheung, Gyeonggi, Korea
E-mail: nanang_mahardika@yahoo.com

**ABSTRAK**

*Makalah ini membahas tentang pengaruh sudut swept (β) terhadap gaya aerodinamik yang dihasilkan oleh Turbin Angin Sumbu Vertikal. Untuk kondisi bilah berputar, koefisien gaya normal ($C_n$) dan koefisien gaya tangensial ($C_t$) dihitung dengan menggunakan metode multiple streamtube model yang berdasarkan Teori Blade Element Momentum. Berdasarkan analisis untuk tiga kondisi tip speed ratio (TSR) yang berbeda, metode multiple streamtube model memberikan hasil perhitungan variasi $C_n$ dan $C_t$ yang mencapai 3,3 kali lebih kecil untuk model bilah dengan β yang tinggi. Di kondisi bilah yang diam, analisis berdasarkan Computational Fluid Dynamics (CFD) dilakukan untuk menghitung variasi gaya torsi yang dihasilkan oleh bilah dengan 12 posisi yang berlainan relatif terhadap arah angin. Perhitungan gaya torsi ini dilakukan untuk 7 model bilah dengan β yang bervariasi. Berbeda dengan hasil dari model matematis Gorlov, CFD memprediksi bahwa gaya torsi rata-rata yang dihasilkan cenderung terus meningkat apabila β dinaikkan. Sementara itu, variasi gaya torsi dapat mencapai 10 kali lebih kecil untuk bilah dengan β yang cukup tinggi.*

***Kata Kunci**: Turbin angin, BEMT, VAWT, CFD, model Gorlov, sudut swept.*

**ABSTRACT**

*This paper discusses the effect of blade's swept angle towards the aerodynamic forces generation of Vertical Axis Wind Turbine (VAWT). In the rotating condition, normal force coefficient ($C_n$) and tangential force coefficient ($C_t$) are calculated by using Blade Element Momentum Theory (BEMT)-based multiple streamtube model. Multiple streamtube model calculation for three different tip speed ratios (TSR) suggests that the variation of $C_n$ and $C_t$ are up to 3.3 times less for the model with higher swept angle. For the startup condition, Computational Fluid Dynamics (CFD) analysis using ANSYS CFX is conducted to calculate the torque variation at twelve different blade positions relative to the wind direction for seven different models. Unlike the Gorlov mathematical model for a helical turbine, CFD analysis predicted that the average torque is increasing as the swept angle increases. Meanwhile, the variation of torque is up to 10 times less for the models with higher swept angle.*

***Keywords:** Wind turbine, BEMT, VAWT, CFD, Gorlov model, swept angle.*

## 1. INTRODUCTION

Global warming and other environmental issues have increased the world awareness of the needs of clean and renewable energy production. As one resource of clean and safe energy, wind power has been extracted and utilized for electricity production since several centuries ago. Nowadays, we can see many kinds of wind harnessing devices are being developed and installed worldwide. These show that a great amount of effort has been poured out and focused on the development of a more efficient wind turbine. A well-known vertical type wind turbine called Darrieus turbine was patented in 1931 by a French engineer. This type of turbine has relatively high efficiency and maximum power can be extracted at lower TSR. However, this turbine has some disadvantages such as low starting torque, the vibration and fatigue problem caused by high normal force ($F_n$) and tangential force ($F_t$) variation at the blades during one cycle of rotation [1-3].

Later in 2001, Gorlov patented a new design that has a similar principle with Darrieus turbine. The most innovative feature of his design is the helical shape of the blade that distributes the airfoil section throughout the rotational cycle. By this way, the blades produce smoother torque and low variation of aerodynamic load and eventually can minimize the blade's vibration. In designing his turbine, Gorlov suggested a mathematical model to calculate the torque at the startup condition. It is assumed that the cross section of the blade has an infinitely thin rectangle. As a consequence, there is an optimum value of airfoil section distribution or the swept angle. For the ratio of blade height to the radius is equal to 2, the optimum swept angle is 74.99˚. The optimum swept angle is described as a function of the ratio of blade height to the radius. In this paper, we demonstrate the effect of changing swept angle of the blade to $C_n$ and $C_t$ by using BEMT-based theory. In addition, we performed CFD analysis to estimate the torque generation. This work is a step toward our final goal that is to develop a small scale turbine with optimum swept, twist and round angle.

## 2. METHODS AND SETUP

There are several analytical methods that have been developed to calculate the performance of Vertical Axis Wind Turbine (VAWT). Some of the methods which are based on BEMT are the single streamtube, multiple streamtube and double-multiple streamtube models. The multiple streamtube was developed by Strickland to predict the velocity distribution across the rotor more precisely than the single streamtube model. In turns, it can predict more accurately the overall performance of turbine [4]. Based on the code simplicity and accuracy, we utilized the multiple streamtube model to examine the variation of $C_n$ and $C_t$ of the blade with different swept angle.

The code is running on MATLAB, 2D airfoil data is acquired from Sheldahl and Klimas model [5] while Viterna-Corrigan formula is used to modify the airfoil data at the post-stall region. Glauert empirical formula [6] is utilized for induction factor larger than 0.4 and flow's Reynolds number is calculated based on relative wind velocity passing the blade [7]. In the code, the blade with swept angle is realized by dividing the blade into many airfoil sections with different initial azimuth angle. Flowchart for multiple streamtube model is shown in Figure 1.

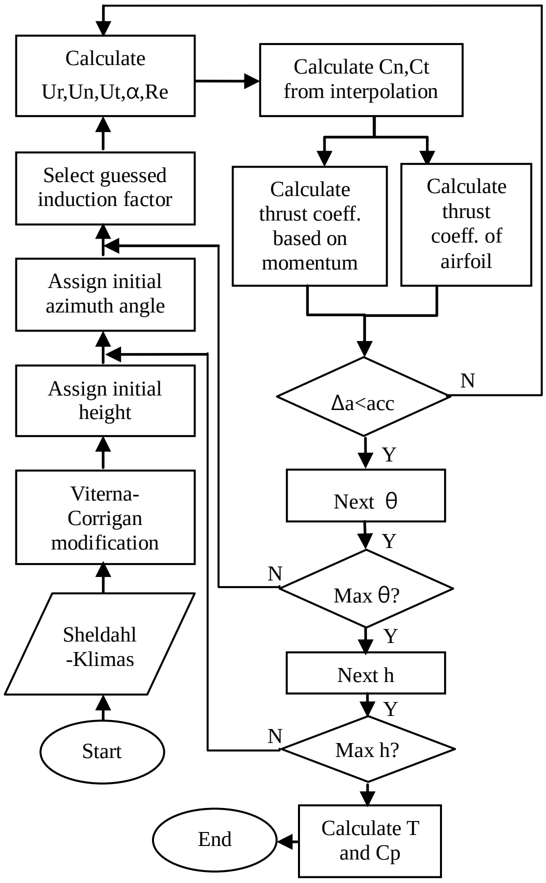


**Figure 1. Multiple streamtube model flowchart**

In addition to the BEMT analysis, CFD analysis is conducted to examine the blade force variation at 12 different blade positions relative to the wind (10˚ difference) for 7 different blade designs. The geometrical data for the blade design is given in Table 1.

**Table 1. Geometrical data of VAWT**

| | |
|---|---|
| Number of blades | 3 |
| Height (m) | 1.04 |
| Diameter (m) | 0.8 |
| Chord Length (m) | 0.12 |
| Airfoil Type | NACA 0015 |
| Solidity | 0.45 |
| Swept angle (˚) | 0˚-200˚ |

Figure 2 shows six of seven models with 0˚, 40˚, 80˚, 120˚, 160˚ and 200˚ of swept angle ($\beta$) which are corresponding to 14.7˚, 21.0˚, 26.3˚, 33.7˚, 45.42˚ and 51.9˚ of sleep angle ($\gamma$), respectively. The schematic of swept ($\beta$) and sleep angle ($\gamma$) are also given in Figure 2.

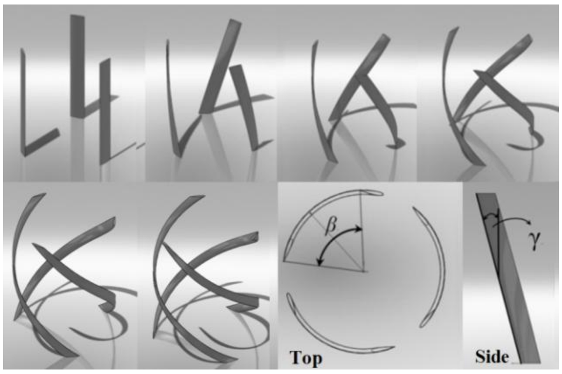


**Figure 2. Blades with 0˚ up to 200˚ of swept angle**

As shown in Figure 3, computational domain is divided into two domains. Domain 1 is the domain where the blades are located. This domain is meshed with tetrahedral and brick-layered hexahedral elements near the blade surface while the height of the first layer of hexahedral is set to have $y^+\approx1$. Domain 2 is meshed with hexahedral elements; uniform free stream velocity (5 m/s) is given at the inlet side while the other sides are a wall and opening pressure boundary conditions with zero relative pressure. The turbulence model used is SST Transitional Gamma-Theta model. The number of elements for domain 1 is 588,715 elements and domain 2 is up to 4,880,655 elements.

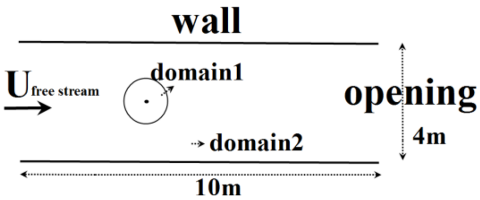


**Figure 3. Scheme of boundary conditions for CFD analysis**

Mesh independency is conducted to assure that the number of the mesh is adequate for estimating the torque. Six different number of mesh is generated for a model with swept angle 0˚. The number of the mesh is varied from 1.2 million to 9.4 million. For the final model, we used mesh generation setting that produces around 4.3 million of elements as shown by a circle in Figure 4. The selection is based on relatively small torque difference compared to the mesh with 9.4 million of elements.

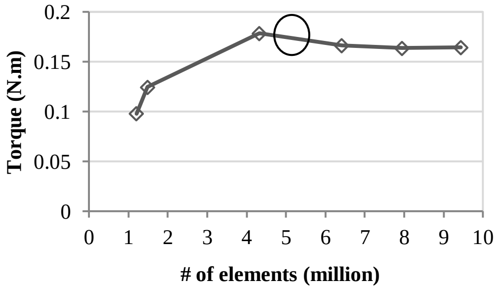


**Figure 4. Mesh independency for model with swept 0˚**

Gorlov developed a mathematical model for design and optimization for helical hydraulic turbine. Even though this model was developed for hydraulic turbine, the same assumption can be applied to a wind turbine. It is assumed that the cross section of the blade has a shape of infinitely thin rectangle with the length equal to airfoil's chord length. Figure 5 shows the schematic of Gorlov model including lines and points that represent the blade and angle definition. Line ADF is representing a blade line while point D is arbitrary point at blade line ADF.

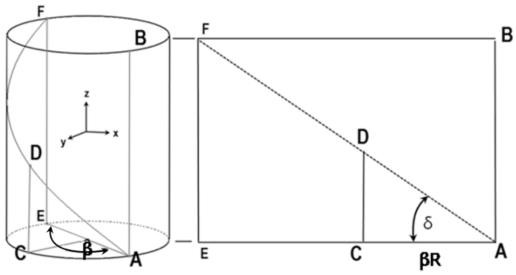


**Figure 5. Gorlov model for helical blade**

$$T = k\sqrt{1+q^2}\, sin^2\left(\frac{L}{Rq}\right) \qquad (1)$$

$$k = \frac{1}{2}1.2\rho R \qquad (2)$$

$$q = tan\,\delta = \frac{L}{\beta R} \qquad (3)$$

The blade's torque is represented by Equation 1, it is a dimensionless representation and a function of blade inclination ($\delta$) or swept angle ($\beta$), while $\rho$ is fluid density, $L$ is the height of blade and $R$ is the radius of blade. In this function, torque reaches maximum values for different swept angle ($\beta$) with changing height to blade's radius ratio ($L/R$). In Figure 6, dimensionless torque as a function of $L/R$ is shown based on Equation 1. For $L/R$=2, maximum torque obtained at swept angle ($\delta$) = 56.8˚ or swept angle ($\beta$) = 74.99˚. For $L/R$=3, maximum torque obtained at swept angle ($\delta$) = 67.6˚ or swept angle

($\beta$) = 70.85°. In the next section, the comparison between Gorlov mathematical model and result from CFD analysis will be shown for *L/R*=2.6.

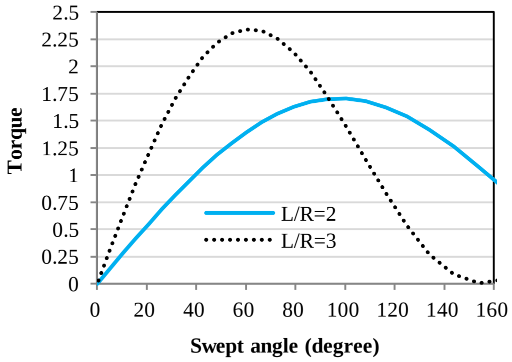


**Figure 6. Startup torque for different L to R ratio (Gorlov model)**

## 3. RESULTS

Calculation for three different solidities ($\sigma$) is conducted to determine the appropriate solidity for the calculation of swept angle effect. As expected, the blades with higher solidity have better performance at low TSR. In the case of TSR=1.5, $C_p$ value for $\sigma$ = 0.65 is 0.20 which is much higher than $C_p$ for $\sigma$ = 0.25 which is only 0.09. Moreover, even though the solidity changed linearly, the optimum *TSR* does not change linearly. As shown in Figure 7, for solidity 0.25, 0.45 and 0.65, the optimum *TSR* are 2, 2.3, and 2.8 respectively. Factors that became our consideration for selecting solidity are that the maximum $C_p$ is decreased 4.84% from 0.347 to 0.33 if we increased solidity from 0.45 to 0.65, but maximum $C_p$ increased only 2.97% to 0.357 if we decreased the solidity to 0.25. Another consideration is that our final design must have a good startup performance which means that higher solidity is preferable.

By comparing the $F_n$ variation, we can predict the effect of solidity to the vibration caused by normal force variation. As shown in Figure 8, BEMT predicts that the maximum $F_n$ at $\sigma$ = 0.65 is up to 160% higher than $\sigma$ = 0.25. If we assume the blades as a simple beam with chord length *c*, the stress can be simplified as a linear function of the second moment of area about one axis which is proportional to the chord length *c*. Therefore, if the solidity is changed by changing the chord length and blades inertial force is neglected, $F_n$ variation has less significant effect since the blades with higher solidity have higher structural strength. Therefore, by considering the efficiency, startup performance and $F_n$ variation, we choose $\sigma$ = 0.45 as the blade solidity for the following CFD analysis.

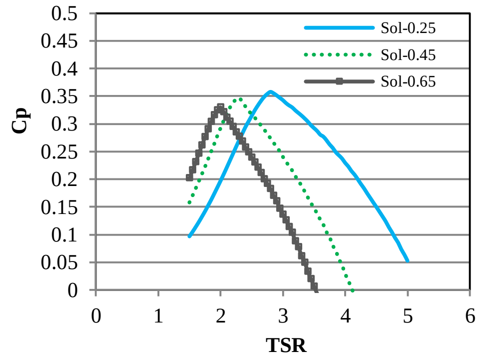


**Figure 7. Cp variation for different solidity**

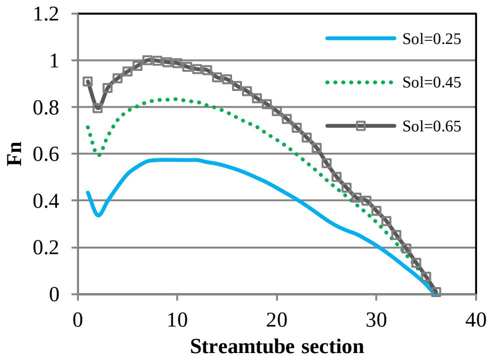


**Figure 8. $F_n$ variation for different solidity**

By using $\sigma$ = 0.45, the effect of changing the swept angle are investigated by observing the standard deviation of $C_n$ and $C_t$ at low, optimum and high TSR. Shown in Figure 9 to Figure 14 are the variation of $C_n$ and $C_t$ for 4 different models with swept angle are 0°, 40°, 80° and 120°. It is obvious implementation of swept angle will change the distribution of $C_n$ and $C_t$ throughout a single rotation. At optimum TSR (2.3), these 4 models have 0.26, 0.22, 0.16 and 0.09 of $C_n$ standard deviation (STD $C_n$). For $C_t$ distribution in terms of standard deviation (STD $C_t$) are 0.044, 0.033, 0.022 and 0.013 for those 4 models, respectively. Complete data of $C_n$ and $C_t$ variation are given in Table 2, the values for low (1.8) and high TSR (2.8) apparently have the same trend with values at optimum TSR. The average $C_n$ (Avg $C_n$) and $C_t$ (Avg $C_t$) are the same, this result is a consequence of assumption that there is no interaction between one blade and another blade element at BEMT theory.

**Table 2. Cn and Ct for different TSR**

| $\beta$ | Avg $C_n$ | Avg $C_t$ | STD $C_n$ | STD $C_t$ |
|---|---|---|---|---|
| *TSR* =1.8 | | | | |
| $\beta$ | Avg $C_n$ | Avg $C_t$ | STD $C_n$ | STD $C_t$ |
| 0˚ | 1.03 | 0.078 | 0.239 | 0.038 |
| 40˚ | 1.03 | 0.078 | 0.202 | 0.034 |
| 80˚ | 1.03 | 0.078 | 0.172 | 0.027 |
| 120˚ | 1.03 | 0.078 | 0.096 | 0.016 |
| *TSR* =2.3 | | | | |
| $\beta$ | Avg $C_n$ | Avg $C_t$ | STD $C_n$ | STD $C_t$ |
| 0˚ | 0.67 | 0.10 | 0.260 | 0.044 |
| 40˚ | 0.67 | 0.10 | 0.224 | 0.033 |
| 80˚ | 0.67 | 0.10 | 0.164 | 0.022 |
| 120˚ | 0.67 | 0.10 | 0.093 | 0.013 |
| *TSR* =2.8 | | | | |
| $\beta$ | Avg $C_n$ | Avg $C_t$ | STD $C_n$ | STD $C_t$ |
| 0˚ | 1.13 | 0.03 | 0.324 | 0.020 |
| 40˚ | 1.13 | 0.03 | 0.254 | 0.017 |
| 80˚ | 1.13 | 0.03 | 0.181 | 0.013 |
| 120˚ | 1.13 | 0.03 | 0.104 | 0.007 |

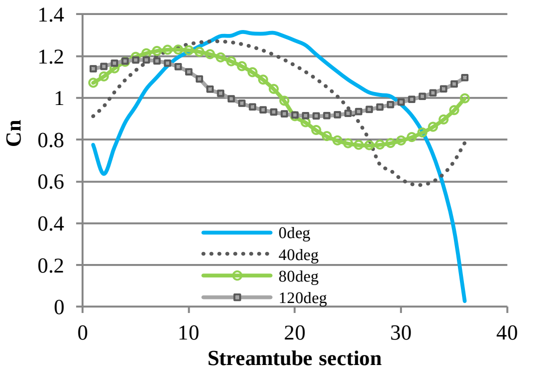


Figure 9. Variation of $C_n$ at low TSR (1.8)

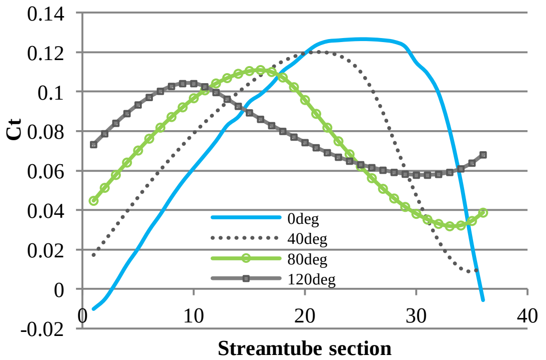


Figure 10. Variation of $C_t$ at low TSR (1.8)

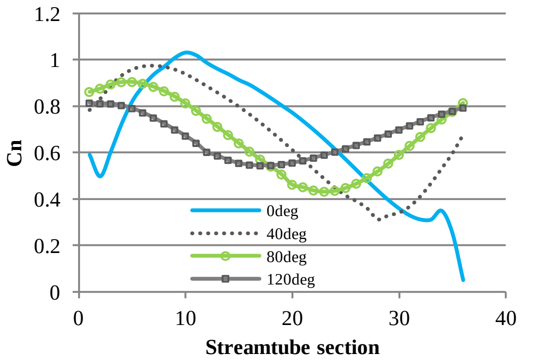


Figure 11. Variation of $C_n$ at optimum TSR (2.3)

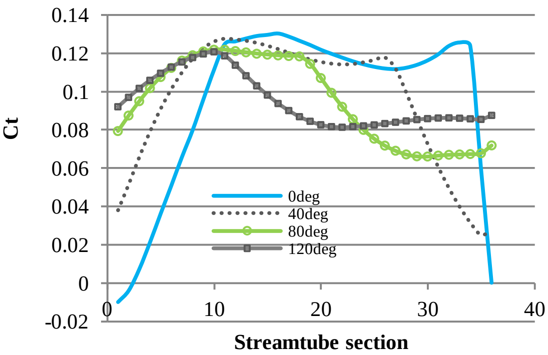


Figure 12. Variation of $C_t$ at optimum TSR (2.3)

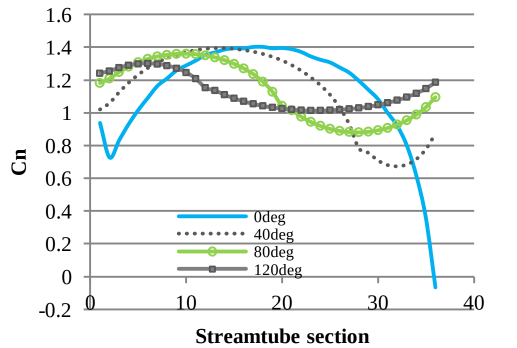


Figure 13. Variation of $C_n$ at high TSR (2.8)

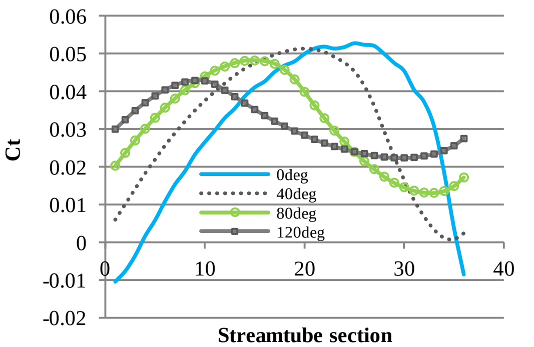


Figure 14. Variation of $C_t$ at high TSR (2.8)

For stationary condition, we investigated the average and the variation of torque by CFD analysis in order to find the best model for startup condition. The simulation is conducted for 7 different models with 0˚, 40˚, 60˚, 80˚, 120˚, 160˚ and 200˚ of swept angle. Torque generations at each position of blade in one rotational cycle are shown in Figure 15 to Figure 20. Average torque calculated by averaging torque generated at those positions (10˚ difference for each rotation).

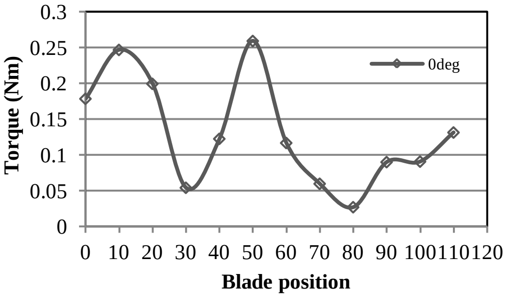


**Figure 15. Variation of torque at model with *β* = 0˚**

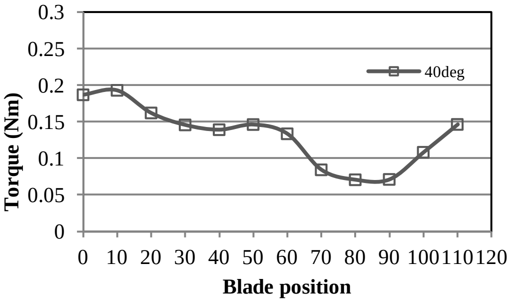


**Figure 16. Variation of torque at model with *β* = 40˚**

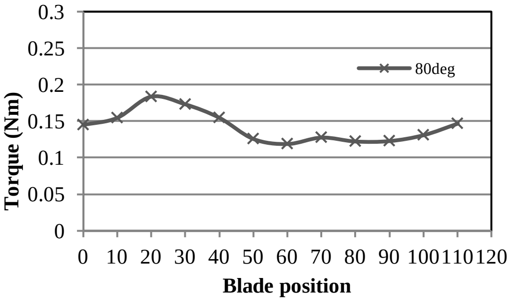


**Figure 17. Variation of torque at model with *β* = 80˚**

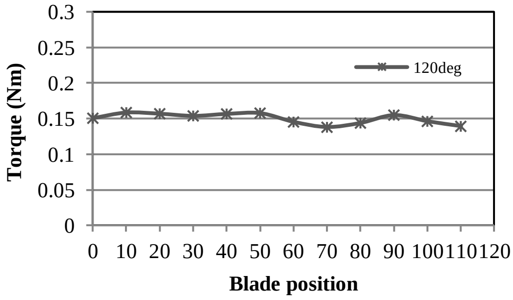


**Figure 18. Variation of torque at model with *β* = 120˚**

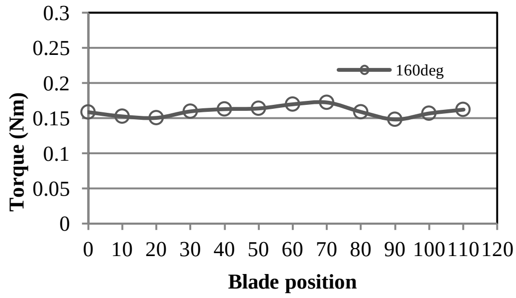


**Figure 19. Variation of torque at model with *β* = 160˚**

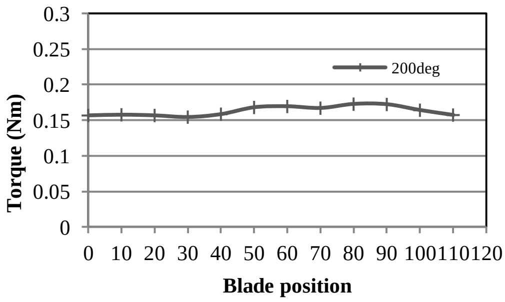


**Figure 20. Variation of torque at model with *β* = 200˚**

Based on the result, the average torque ($T_{avg}$) generated are ranging from 0.1307 Nm to 0.1630 Nm. The standard deviation ($STD$-$T_{avg}$) are also given in Table 3. The average torque tends to increase as the swept angle increase except for 40˚ of swept angle as shown in Figure 22. The increment ($\Delta T$) is up to 19.46%. Based on the calculation of torque standard deviation ($\Delta STD$), the variation of torque can be reduced up to 10 times. However, the reduction becomes smaller for the blade with swept angle higher than 120˚ as shown in Figure 23. For startup performance, more uniform torque value is preferable to overcome static friction of turbine under static condition. In any position where the blade's torque is higher than the static friction, the turbine should be easily rotated.

**Table 3. Average and standard deviation torque by CFD**

| $\beta$ | $T_{avg}$ | $\Delta T$ | $STD\text{-}T_{avg}$ | $\Delta STD$ |
|---|---|---|---|---|
| 0˚ | 0.1312 | - | 0.0719 | - |
| 40˚ | 0.1307 | 0.56% | 0.0394 | -0.8 |
| 60˚ | 0.1402 | 5.02% | 0.0296 | -1.4 |
| 80˚ | 0.1419 | 7.80% | 0.0202 | -2.6 |
| 120˚ | 0.1514 | 12.76% | 0.0071 | -9.1 |
| 160˚ | 0.1600 | 17.97% | 0.0069 | -9.4 |
| 200˚ | 0.1630 | 19.46% | 0.0064 | -10.2 |

As described in the previous section, Gorlov developed a mathematical model for helical shape blade (with swept angle). Based on Equation 1, for *L/R*=2.6, we plotted the torque as a function of swept angle as shown in Figure 21.

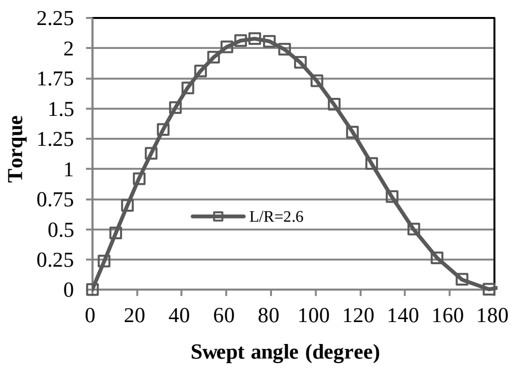


**Figure 21. Startup torque based on Gorlov model for different *β***

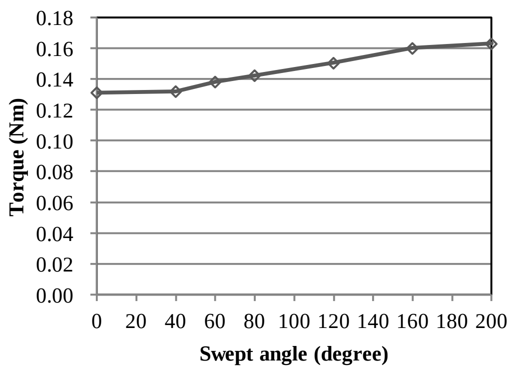


**Figure 22. Startup torque based on CFD for different *β***

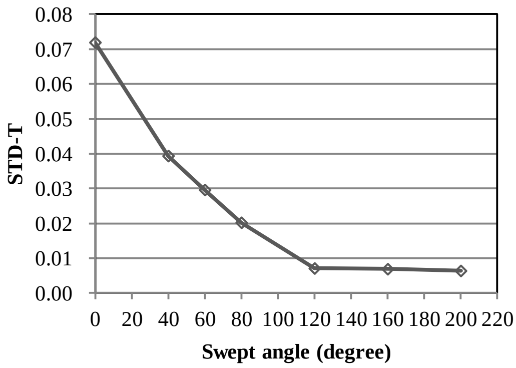


**Figure 23. Startup torque variation based on CFD for different *β***

Under assumptions and condition described in this paper, there is large difference between Gorlov model and CFD result in torque generation. In the Gorlov model (Figure 21), maximum torque occurs at swept angle ($\beta$) = 64˚ and decreases as the swept angle increases while the average torque by CFD increases as the swept angle increases shown in Figure 22.

## 4. SUMMARY

In this works, we have investigated the effect of implementing swept angle to the blade. In the first part, we utilized BEMT to predict average $C_n$ and $C_t$ and its variation in terms of standard deviation. The result predicts that the variation of $C_n$ and $C_t$ can be reduced up to 3.3 times for model with 120˚ of swept angle. However, the average $C_n$ and $C_t$ are the same for the model with different swept angle. This result is a consequence of the assumption that BEMT calculates the aerodynamic force for each section of blade's airfoil without considering 3D effect of the flow. The effect of blade solidity to the variation of $F_n$ is also briefly described. As the solidity increased by changing the chord length of airfoil, the structural strength is increased as well. Therefore, for our interest, less consideration for solidity is given compared to the other variable such as swept angle. Based on efficiency and startup performance, we selected blade's solidity of 0.45. In the second part, CFD analysis was conducted to analyze 7 different models with different swept angle by calculating the torque generation for 12 different positions of blade. The average torque tends to increase as the swept angle increases; the difference is up to 19.46 % for model with higher swept angle. In addition to the larger blade surface area, such increase of torque might be attributed to 3D flow effect where the flow from upper section of the blade influences the air flow at lower sections. Meanwhile, the torque variation can be reduced up to 10 times. The calculation based on Gorlov model shows that the optimum swept angle for $L/E$ = 2.6 is 64˚, while CFD predicts that torque keeps increasing for swept angle more than 64˚. These results suggest that there is a significant 3D effect for implementing the swept angle. In addition to gain a better understanding of how this 3D effect influences the aerodynamic force generation, further simulation and experimental investigation are needed to validate the results of this preliminary analysis.

## REFERENCES


[1] Popelka D, Aeroelastic Stability Analysis of a Darrieus Wind Turbine, SANDIA Report, 1982.

[2] Abdel Azim A.F., Hirsch C, Derdelinckx R, Dynamics of Vertical Axis Wind Turbine, International Journal of Rotating Machinery, 1995.

[3] Tangler J L, The Evolution of Rotor and Blade Design, American Wind Energy Association Wind Power, 2000.

[4] Strickland J H, The Darrieus turbine: A performance prediction model using multiple streamtubes, SANDIA, 1975.

[5] Sheldahl R.E, Klimas P.C, Aerodynamics Characteristics of Seven Symmetrical Airfoil Sections Through 180 degree Angle of Attack for Use in Aerodynamic Analysis of Vertical Axis Wind Turbine, 1981.

[6] Moriaty P J, Hansen A C, AeroDyn theory Manual, 2005.

[7] Lian, D, Lee J H, Kim Y C, Power Prediction of Darrieus Type Wind Turbine Considering Real Air Velocity On the Wind Turbine Blade.